Effects of Proinflammatory Cytokines on the Claudin-19 Rich Tight Junctions of Human Retinal Pigment Epithelium

Shaomin Peng,[1–3] *Geliang Gan,*[1,3] *Veena S. Rao,*[3] *Ron A. Adelman,*[3] *and Lawrence J. Rizzolo*[1,3]

Purpose. Chronic, subclinical inflammation contributes to the pathogenesis of several ocular diseases, including age-related macular degeneration. Proinflammatory cytokines affect tight junctions in epithelia that lack claudin-19, but in the retinal pigment epithelium claudin-19 predominates. We examined the effects of cytokines on the tight junctions of human fetal RPE (hfRPE).

Methods. hfRPE was incubated with interleukin 1-beta (IL-1β), interferon-gamma (IFNγ), or tumor necrosis factor-alpha (TNFα), alone or in combination. Permeability and selectivity of the tight junctions were assessed using nonionic tracers and electrophysiology. Claudins, occludin, and ZO-1 were examined using PCR, immunoblotting, and confocal immunofluorescence microscopy.

Results. Only TNFα consistently reduced transepithelial electrical resistance (TER) >80%. A serum-free medium revealed two effects of TNFα: (1) decreased TER was observed only when TNFα was added to the apical side of the monolayer, and (2) expression of TNFα receptors and inhibitors of apoptosis were induced from either side of the monolayer. In untreated cultures, tight junctions were slightly cation selective, and this was affected minimally by TNFα. The results were unexplained by effects on claudin-2, claudin-3, claudin-19, occludin, and ZO-1, but changes in the morphology of the junctions and actin cytoskeleton may have a role.

Conclusions. Claudin-19–rich tight junctions have low permeability for ionic and nonionic solutes, and are slightly cation-selective. Claudin-19 is not a direct target of TNFα. TNFα may protect RPE from apoptosis, but makes the monolayer leaky when it is presented to the apical side of the monolayer. Unlike other epithelia, IFNγ failed to augment the effect of TNFα on tight junctions. (*Invest Ophthalmol Vis Sci.* 2012;53:5016–5028) DOI:10.1167/iovs.11-8311

Age-related macular degeneration and proliferative diabetic retinopathy are among the leading causes of blindness and visual impairment in the United States. An important element of these diseases is a low grade, subclinical inflammatory process.[1] Proinflammatory cytokines, such as interleukin-1-beta (IL-1β), interferon-gamma (IFNγ), and tumor necrosis factor-alpha (TNFα) have been implicated in these and other ocular diseases.[1–9] These diseases may alter the blood-retina barrier through effects on tight junctions.[10–12] Tight junctions retard transepithelial diffusion of solutes via the spaces that lie between neighboring cells of the RPE or capillary endothelial cells.[13]

RPE is a simple, transporting epithelium that lies between the neural portion of the retina and the fenestrated choriocapillaris. Apical microvilli of RPE interdigitate with photoreceptor outer segments in the subretinal space. RPE pumps water out of this space to maintain this close association. The ion gradients needed to support transepithelial transport depend on cooperative interactions between membrane transporters and tight junctions.[13] Cytokines can act on both components of the blood-retinal barrier.

Inflammatory cells, endothelia, and activated RPE may release a plethora of inflammatory mediators that may induce progressive pathologic changes in the retina and RPE. IL-1β decreased the transepithelial electrical resistance (TER) of ARPE19 cells directly or indirectly through effects on tight junction proteins.[14] In human fetal RPE (hfRPE), a cocktail of these cytokines affected the polarized secretion of cytokines/chemokines and decreased TER after 24 hours, but increased rapidly net epithelial fluid absorption.[15,16] Most of the effect on fluid absorption was attributed to IFNγ effects on Cl^- transport.

IL-1β, IFNγ, and TNFα regulate epithelial and endothelial tight junctions in vivo and in vitro, but the effects are tissue-specific. TNFα decreased TER and increased paracellular permeability in several cell lines,[17–19] but not others.[20] IFNγ caused a dose- and time-dependent increase in monolayer permeability of colon cultures,[21,22] but it also decreased permeability in murine endothelia, and enhanced barrier function and wound healing in lung cell culture.[23,24] IFNγ can act synergistically with TNFα to increase paracellular permeability.[20,25,26] There is little information on how cytokines affect the selectivity of tight junctions.

The permeability and selectivity of tight junctions are determined by the claudin family of transmembrane proteins and may be modulated by occludin (see review of Rizzolo et al.[13]). Of the 24 known claudins, hfRPE expressed predominantly claudin-19 with lesser amounts of claudin-3.[27] Claudin-19 also is prominent in adult RPE.[28,29] Absence of functional claudin-19 results in a loss of TER in culture and severe visual

From the [1]Department of Surgery, Yale University School of Medicine, New Haven, Connecticut; [2]Department of Ophthalmology, Second Affiliated Hospital of Harbin University, Harbin, China; and [3]Department of Ophthalmology, Yale University School of Medicine, New Haven, Connecticut.

Supported by the National Eye Institute vision core Grant EY000785 (Yale University), Research to Prevent Blindness (Yale Department of Ophthalmology), the International Retinal Research Foundation (LJR), Connecticut Innovations 10SBC02 (LJR), the Leir Foundation (RAA), the Newman's Own Foundation (RAA), the National Natural Science Foundation of China No. 30772381 (SP), and the Yale Endowed Student Research Fellowship (VSR).

Submitted for publication July 28, 2011; revised November 21, 2011 and June 8, 2012; accepted June 25, 2012.

Disclosure: **S. Peng**, None; **G. Gan**, None; **V.S. Rao**, None; **R.A. Adelman**, None; **L.J. Rizzolo**, None

Corresponding author: Lawrence J. Rizzolo, Department of Surgery, Yale University School of Medicine, PO Box 208062, New Haven, CT 06520-8062; lawrence.rizzolo@yale.edu.

Investigative Ophthalmology & Visual Science, July 2012, Vol. 53, No. 8

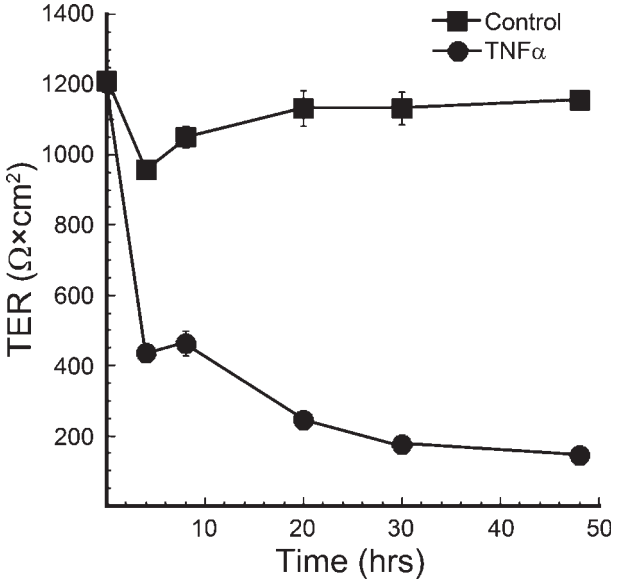

Figure 1. Time course for the effects of TNFα. Cells maintained in growth medium were incubated with growth medium containing 0.5% FBS for 24 hours before TNFα or vehicle was added to both media chambers (*time 0*). The TER was monitored using Endohm electrodes. *Error bars*: the SE estimated from three cultures. Some error bars are smaller than the symbol.

defects in patients.[27,30] In contrast, claudin-3 does not make a measurable contribution to the properties of the tight junction. Whereas knockdown of claudin-3 by siRNA has no discernible effect, a knockdown of claudin-19 virtually eliminates the TER.[27] Knockdown of claudin-19 fails to alter the expression or subcellular localization of claudin-3, which indicates the amount of claudin-3 present in RPE is incapable of forming a functional tight junction on its own. Although the gene for claudin-3 is in the locus for Williams-Beuren syndrome, the ocular defects associated with this disease are attributed to other genes in that locus.[31,32] Besides claudin-3 and claudin-19, trace amounts of the mRNAs for claudin-1, claudin-2, claudin-10, claudin-12, claudin-15, claudin-16, and claudin-20 also were reported. These same proteins and mRNAs were expressed in vivo and in cultured hfRPE. Notably, claudin-19 has not been reported in ARPE19, a cell line that often is used to study RPE tight junctions.

Previous studies examined the effects of brief exposures to TNFα, IL-1β, or IFNγ on hfRPE barrier properties, and found little evidence of effects on the paracellular pathway.[15,16] To investigate whether longer exposures to these cytokines had an effect on tight junctions, we used two culture models: one in which hfRPE was maintained in a serum-containing medium, and one in which hfRPE was adapted to a serum-free medium (SFM-1). We were concerned about how serum might affect our results for two reasons. Serum contains variable mixtures of factors that might modulate the effects of cytokines, and serum on the apical side of the RPE increases TER to hyperphysiologic levels.[27] Commonly, the first issue is addressed by preincubating the cultures in serum-reduced or serum-free medium. Using TER as in indicator, we found that RPE could be maintained for extended periods in reduced-serum medium, but a specialized media formulation was required to maintain RPE in a serum-free medium.[27] In SFM-1, the TER decreased gradually to more physiologic levels over the course of four weeks. After this transition period, the cultures became stable, and the process could be reversed by returning the cultures to serum-based medium. In both media, hfRPE is highly differentiated and exhibits many of the functions expected for native RPE.[27,33–35] This strategy allowed us to relate our results to previous studies with hfRPE cultures,[15,16] and examine stable cultures of RPE in serum-free conditions.[27]

Our current study quantified the permeability and selectivity of RPE tight junctions, and how these properties are affected by this group of cytokines. We also reported on whether these cytokines affected mRNA and protein expression, and the cellular distribution, of claudins and occludin. The study led us to focus on the effects of TNFα.

Methods

Cell Culture

This research followed the tenets of the Declaration of Helsinki, the institutional review board of the National Institutes of Health, and Yale

Table 1. Effect of Cytokines on the TER

	GM 0.5%						SFM-1					
Donor	**1**	**2**	**3**	**4**	**5**	**6**	**1**	**2**	**3**	**4**	**5**	**6**
% of control TER												
Cytokine												
TNFα	16.5	14.7	8.1	19.5	17.1	–	25.9	33.3	14.2	8.5	5.4	–
IL-1β	86.5	93.3	101.3	103.8	96.8	–	93.4	100.4	103.8	105.2	103.9	–
IFNγ	93.9	82.4	101.4	118.5	119	–	68.1	94.1	104.7	108.7	112.5	–
TNFα + IL-1β	–	–	–	15.8	9.6	19	–	–	–	7.5	6.6	15.8
TNFα + IFNγ	–	–	–	12.6	14.4	15.8	–	–	–	8.3	8.1	15.3
TNFα + IL-1β + IFNγ	–	–	–	8.4	10.2	17.3	–	–	–	8.4	7.5	9.3
TER (Ω × cm²)												
Control	1301	1041	1491	918	822	834	453	479	887	629	670	430

Experiments were performed after the cultures attained a stable TER as described.[27] Cells were incubated for 48 hours in the indicated cytokine. Measurements were made in culture medium using the EVOM resistance meter at ambient temperature. The actual TER is reported for the control cells, but the TER as a percentage of the control was shown for each test condition. For each preparation, the TER is the average of three cultures. SE was less than 5%.

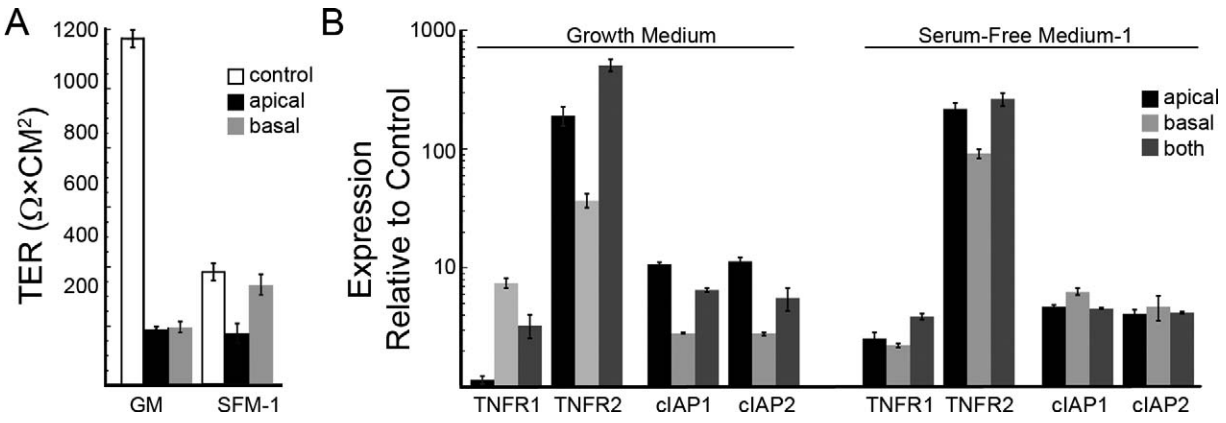

Figure 2. Polarity of the effects of TNFα. TNFα was added to the apical, basal, or both media chambers for 48 hours. (**A**) In growth medium, the TER was reduced regardless of which medium chamber contained TNFα, but in SFM-1 the TER was significantly reduced only if TNFα was added to the apical medium chamber. (**B**) Expression of TNFα receptors and cIAP was monitored by qRT^2-PCR. For each mRNA, expression relative to that mRNA in control cultures was calculated as described in the methods. (10 = 10× increase due to the cytokine). TNFR1 mRNA was detected readily in control cells. For cultures maintained in growth medium, TNFR1 expression was affected only when TNFα was added to the basal medium chamber. For cultures maintained in SFM-1, TNFα increased expression from either chamber. In control cultures, TNFR2 mRNA was evident only in trace amounts. The effect of TNFα was nonpolarized in each culture. The effect of TNFα was also nonpolarized for cIAP1 and cIAP2.

School of Medicine guidelines. The primary cultures of hfRPE cells (15–16 weeks' gestation) were supplied by the laboratory of Sheldon Miller (National Eye Institute, Bethesda, MD) and were reseeded, 1.3×10^5 cells per well, onto Transwell or Snapwell culture inserts (1.12 cm^2 growth area, 0.4 μm pores; Corning, Inc., Corning, NY), as described.[27] We refer to the medium formulated by the Miller laboratory as "growth medium." Once a monolayer of RPE forms, the culture insert divides the medium into two chambers, apical and basolateral media chambers. For serum-free medium experiments, cultures were adapted to SFM-1, which also has been used to culture hfRPE.[27,35] MDCK II cells were obtained from the American Type Culture Collection (Manassas, VA) and cultured in Dulbecco's modified Eagles medium (DMEM) containing 5% fetal bovine serum (FBS).

Incubation with Cytokines

Once the TER was stable, we found that the serum in growth medium could be reduced to 0.5% with no discernible effect. This reduced serum formulation was used for all experiments in growth medium that are reported in this study. Similar results were obtained in growth medium containing 5.0% or 0.0% serum (data not shown). For experiments performed in growth medium, the serum was reduced to 0.5% 1.0 hour before the experiment. Parallel experiments were performed in serum-free adapted cultures. Cultures were incubated for two days in media containing the following cytokines, alone or in combination: TNFα 10 ng/ml, IL-1β 10 ng/mL (Sigma-Aldrich, St. Louis, MO), and IFNγ 5 ng/mL (PeproTech, Rocky Hill, NJ). The cytokines were added to both media chambers, or just to the apical or basolateral medium chamber. These concentrations conformed to earlier studies with hfRPE.[15,16]

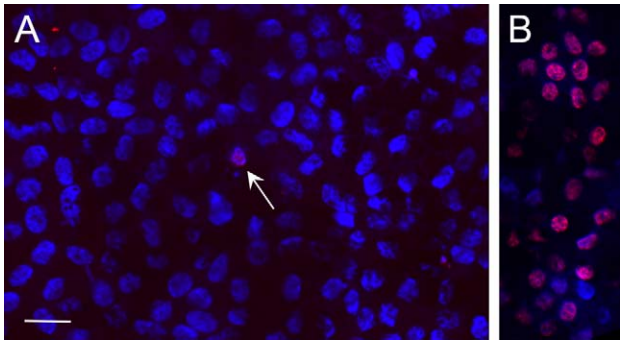

Figure 3. Apoptosis was minimal after a 48-hour exposure to TNFα (**A**) Cultures maintained in SFM-1 were incubated with TNFα and labeled using the TUNEL procedure to reveal apoptotic cells. Nuclei were labeled blue by DAPI. Only the occasional microscopy field exhibited a positive cell (*arrow*), which is purple due to the colocalization of nuclei with the TUNEL reaction product (*false colored red*). Similar results were obtained in growth medium. (**B**) As a positive control, cells were treated with DNase I to create a substrate for the TUNEL assay. Most nuclei were *purple*. *Bar*: 20 μm.

Apoptosis Assay

A TUNEL assay, In Situ Cell Death Detection Kit, Fluorescein (Roche Diagnostics Corp., Indianapolis, IN) was used to detect apoptosis based on labeling of DNA strand breaks by terminal deoxynucleotidyl transferase. For a positive control, fixed and permeabilized cultures were treated with recombinant DNase I (Roche Diagnostics Corp.) for 10 minutes at room temperature to induce DNA strand breaks. Samples were analyzed by confocal fluorescence microscopy, as described below.

Measurement of TER and Ion Selectivity

To monitor hfRPE cultures, the TER was measured at ambient temperature using an EVOM resistance meter with Endohm electrodes (World Precision Instruments, Sarasota, FL) in growth medium or serum-free medium and reported as $\Omega \times \text{cm}^2$. The TER is related to the resistance of the tight junctions (the paracellular or shunt resistance), and the resistances of the apical and basolateral membranes by the following equation:

$$TER = R_S \times \left(\frac{R_A + R_B}{R_A + R_B + R_S} \right) \quad (1)$$

where R_S is the shunt resistance, R_A is the resistance of the apical membrane, and R_B is the resistance of the basolateral membrane.[36] The TER approximates the resistance of the tight junctions when:

$$(R_A + R_B) \gg R_S \quad (2)$$

and

$$\left(\frac{R_A + R_B}{R_A + R_B + R_S} \right) \approx 1 \quad (3)$$

Table 2. Effect of Cytokines on Ion Selectivity

Culture Medium	Apparent R_{tj} ($\Omega \times cm^2$)*	TEP† (mV)	Permeation Coefficient ($P \times 10^6$cm/sec)			Permeation Ratio		
			Na^+	K^+	Cl^-	Na^+/Cl^-	K^+/Cl^-	K^+/Na^+
GM								
Control	560 ± 90	0.23 ± 0.08	2.3 ± 0.3	2.9 ± 0.4	2.4 ± 0.3	0.93 ± 0.02	1.19 ± 0.03	1.28 ± 0.03
TNFα	50 ± 5‡	−0.03 ± 0.01‡	26 ± 3‡	32 ± 3‡	25 ± 3‡	1.06 ± 0.02	1.29 ± 0.03	1.21 ± 0.01
IFNγ	410 ± 20	0.6 ± 0.2	2.9 ± 0.1	3.8 ± 0.2	3.1 ± 0.1	0.94 ± 0.01	1.23 ± 0.02	1.31 ± 0.02
SFM-1								
Control	330 ± 20	0.31 ± 0.03	3.9 ± 0.3	4.9 ± 0.3	3.5 ± 0.3	1.11 ± 0.01	1.38 ± 0.03	1.25 ± 0.02
TNFα	59 ± 6‡	0.05 ± 0.04‡	22 ± 2‡	27 ± 3‡	21 ± 3‡	1.06 ± 0.01	1.28 ± 0.01	1.21 ± 0.01
IFNγ	270 ± 10‡	0.77 ± 0.08	4.9 ± 0.2	6.8 ± 0.3	4.4 ± 0.1	1.11 ± 0.02	1.55 ± 0.05	1.39 ± 0.02
Bare filter	5.6 ± 0.1	0.01 ± 0.01	188 ± 4	233 ± 4	245 ± 4	0.77 ± 0.01	0.95 ± 0.01	1.24 ± 0.01

Measurements were made in triplicate using an Ussing chamber maintained at 37°C. Data are shown for a donor in which IFNγ had a small effect. The results shown for TNFα are representative of all donors. The permeation coefficient was calculated as described in Methods. Representative experiments are shown in Figure 3. The SE is indicated and was estimated from three cultures.

* Because membrane transporters were inhibited, the resistance of the tight junctions was estimated from the TER according to equations (*1*)–(*3*) in Methods.

† In the presence of membrane transport inhibitors (TEP ≈ 1–2 mV without inhibitors).

‡ $P < 0.05$ compared to the control.

This condition likely does not hold for hfRPE, which means the TER underestimates the resistance of the tight junctions.

To measure tight junction-specific properties, cultures maintained on Snapwell filters were mounted in Ussing chambers (Physiologic Instruments, San Diego, CA) and incubated in a modified Ringer's solution to inhibit membrane transport. The solution contained 150 mM NaCl, 2 mM $CaCl_2$, 1 mM $MgCl_2$, 3 mM $BaCl_2$, 10 mM glucose, and 10 mM HEPES, pH 7.4 at 37°C, and continuously bubbled with compressed air. The $BaCl_2$ was sufficient to reduce diffusion through K^+ channels even in those experiments in which KCl was substituted for NaCl.[37–39] The lack of bicarbonate would reduce diffusion through bicarbonate transporters, thereby inhibiting a major transport system in RPE.[40] The assumption that transmembrane ion transport was inhibited substantially was verified by demonstrating that the transepithelial electrical potential (TEP) was reduced from ~2.0 mV to near zero, and the TER increased as predicted by equation (*1*).

Silver chloride electrodes with 3 M KCl agar bridges were used for the current producing and voltage sensing electrodes, and were controlled by a model VCC MC6 voltage/current clamp and ACQUIRE & ANALYZE Revision II software (Physiologic Instruments). The TEP was referenced to the basolateral chamber. For ion selectivity and permeability, dilution and bi-ionic electrical potentials were examined by replacing the solution in the basolateral chamber. Several experiments were performed by replacing the solution in the apical chamber to confirm that the measurements were independent of the direction of the gradient. For dilution potentials, the NaCl in the basolateral was reduced to 75 mM NaCl and the osmolality was balanced with mannitol. For bi-ionic potentials, the NaCl was replaced with 150 mM KCl.

The relative ionic permeabilities of the monolayers were calculated using the Goldman-Hodgkin-Katz equation. The individual permeation coefficients for Na^+ (P_{Na}), Cl^- (P_{Cl}) and K^+ (P_K) were deduced from the method of Kimizuka and Koketsu using the following equations.[41,42]

$$V_{dilution} = -\frac{RT}{F} \times \ln\left(\frac{\alpha + \beta}{1 + \alpha\beta}\right) \quad (4)$$

$$P_{Na} = \frac{RT}{F^2} \times \frac{G_m}{A(1 + \beta)} \quad (5)$$

$$V_{bi-ionic} = \frac{RT}{F} \times \ln\left(\frac{\lambda + \beta}{1 + \beta}\right) \quad (6)$$

where R and F are the gas and Faraday constants, respectively; T is the temperature in °K; α is the activity ratio of NaCl in 150 mM and 75 mM solution; β is permeability ratio, Cl^-/Na^+; G is the conductance (1/TER) per unit surface area; A is the NaCl activity in 150 mM solution; and λ is the permeability ratio, K^+/Na^+. The mean activity coefficient of each monovalent cation-halide salt was assumed to be the same as that of NaCl, and the anion and cation in each case were assumed to have the same activity coefficient.

Paracellular Flux of Methylpolyethylene Glycol (mPEG)

The paracellular flux of mPEG (average molecular weight, 550; Stokes radius = 5.1 Å; MP Biomedicals, LLC, Solon, OH) was estimated as described.[27] Briefly, mPEG, was added to the basal medium chamber to a final concentration of 50 μg/ml. The cultures were incubated for 1.5 hours at 37°C in a humidified chamber with 5% CO_2, and the medium from the apical medium chamber collected for analysis.

Quantitative, Reverse Transcriptase, Real Time-PCR (qRT^2-PCR)

For analysis by agarose gel electrophoresis, RT-PCR was performed as described,[34] using 35 cycles of PCR. qRT^2-PCR was performed as described.[27] Relative expression of mRNA was calculated using the $2^{-\Delta\Delta C_T}$ method.[43] Using this method, data were normalized to glyceraldehyde-3-phosphate dehydrogenase and compared to the respective claudin's mRNA expression in a control, as noted in each figure.

Protein Electrophoresis and Immunoblotting

Electrophoresis and immunoblotting were performed as described.[27] The following primary antibodies were used: rabbit polyclonal anti-claudin-1, rabbit polyclonal anti-claudin-2, rabbit polyclonal anti-claudin-3, mouse monoclonal anti-claudin-10, mouse monoclonal anti-occludin, mouse monoclonal anti-α-tubulin, mouse anti-ZO-1 (Invitrogen, Carlsbad, CA), and rabbit polyclonal anti-claudin-19 (a kind gift from Mikio Furuse, Kobe University, Kobe, Japan).

Immunofluorescence and Confocal Microscopy

The subcellular distribution of claudins, ZO-1, and occludin was determined by indirect immunofluorescence, as described.[27] The primary antibodies listed above were used followed by incubation with ML-grade secondary antibodies conjugated with Cy3 or Cy5 dyes

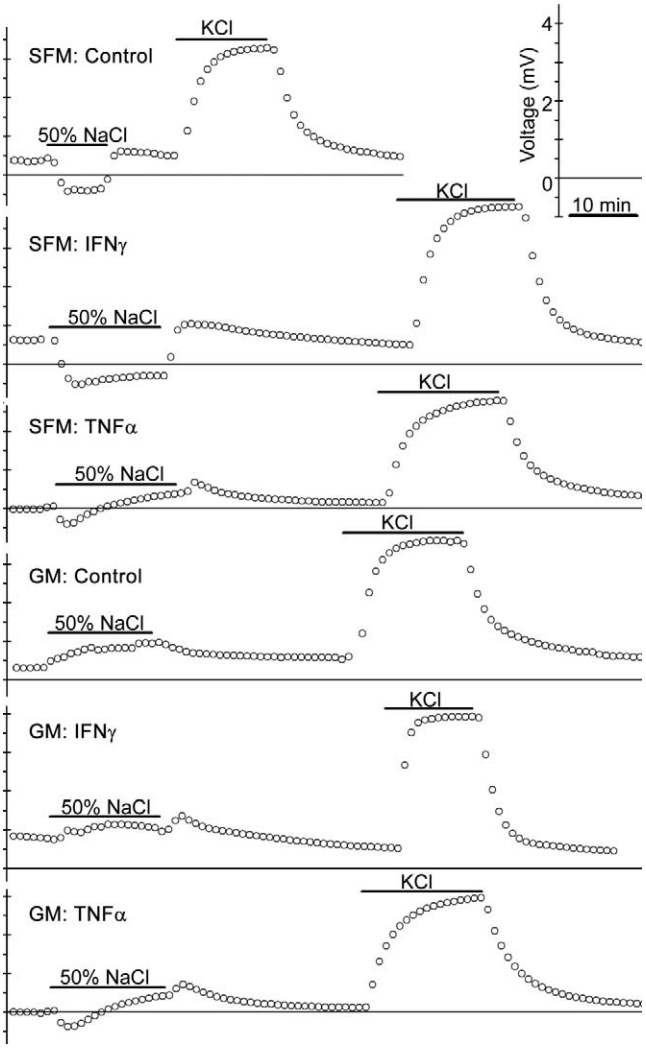

Figure 4. Dilution and bi-ionic electrical potentials for hfRPE maintained in cytokines. Cells were cultured in SFM-1 or growth medium (GM) in the indicated cytokine for two days and transferred to an Ussing chamber in a buffered saline solution containing NaCl, as described in Methods. The presence of $BaCl_2$ and absence of bicarbonate reduced the TEP to near zero. Solutions were changed on the basal side of the culture and measurements were referenced to the basolateral chamber. *Bars*: indicate the duration of the exposure of the culture to reduced NaCl or KCl. Reintroduction of the normal NaCl solution restored the TEP to baseline. When the NaCl concentration was reduced, a negative potential would indicate selectivity for Na^+. When the NaCl was replaced by KCl a positive potential would indicate selectivity for K^+. Data were acquired at 10-second intervals; 1.0-minute intervals are indicated by the *data points* on the graph. Each trace is representative of three experiments. The data were used to calculate the permeation coefficients listed in Table 2.

(Jackson ImmunoResearch Laboratories, West Grove, PA). Alexa Fluor 488 phalloidin was used to label F-actin and DAPI was used to label the nucleus. Fluorescence images were acquired with an LSM 410 spinning-disc confocal microscope and processed using AxioVision software to produce a maximum intensity projection (MIP) or a three-dimensional rendering (Carl Zeiss, Inc., Thornwood, NY). To create an MIP rendering, each image of the confocal stack of images is superimposed and the fluorescent signal from each image is summed together. This procedure compensates for the waviness of the filter and allows junctions from all the cells to be observed simultaneously in a large microscopic field. Fluorescent channels were captured in gray scale and false-colored using the software, as described in the figure legends.

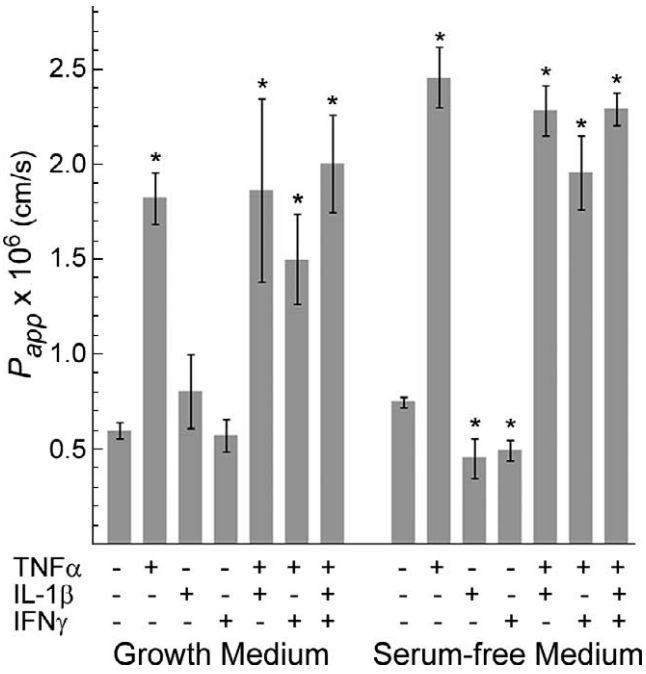

Figure 5. Effect of cytokines on the permeation of PEG_{550}. Cultures were incubated with the indicated cytokines for 48 hours. Similar results were obtained in GM and SFM-1. Only TNFα increased the apparent permeation coefficient (P_{app}). There was no statistical difference among any of the conditions that included TNFα. When 5 mM EDTA was used to disrupt tight junctions, $P_{app} = 6.7 \pm 0.8 \times 10^{-6}$ cm/s. *Bars*: represent the average of 4 to 9 cultures. *Error bars*: represent the SE. $^*P < 0.05$ compared to the control for the corresponding culture medium.

Small Interfering RNA (siRNA)

To knockdown the expression of claudin mRNA, we used a pool of 4 siRNAs specific for either claudin-2 or claudin-4 (siGENOME SMART-pool; Dharmacon, Lafayette, CO) according to the manufacturer's protocol.[27] Transfection with siRNAs specific for claudin-4 served as a negative control because claudin-4 is not expressed by hfRPE. To monitor the effect on mRNA and protein, cells transfected with siRNA were harvested 5, 7, 9, and 11 days post-transfection. Based on these experiments, the effect of TNFα on cells with claudin-2 knocked down was measured by first transfecting the cells and subsequently treating them with TNFα 8 days post-transfection. Cells then were harvested 2 days later for analysis.

Overexpression of Claudin

hfRPE cultured on Transwell or Snapwell filters in SFM-1 were infected by 5×10^8 PFU/well human adenovirus-CLDN2, (SignaGen Labratories, Gaithersburg, MD) in 400 μL. Adenoviral vector that expressed green fluorescence protein (GFP) was used as a control. Cultures were maintained for 48 hours before analysis.

Statistical Analysis

Statistical differences were determined using Student's *t*-test or one-way ANOVA using a Student-Newman-Keuls post-test.

Results

A time course showed that TNFα decreased TER after 4 hours and exerted its maximal effect after 24 hours (Fig. 1). After 48

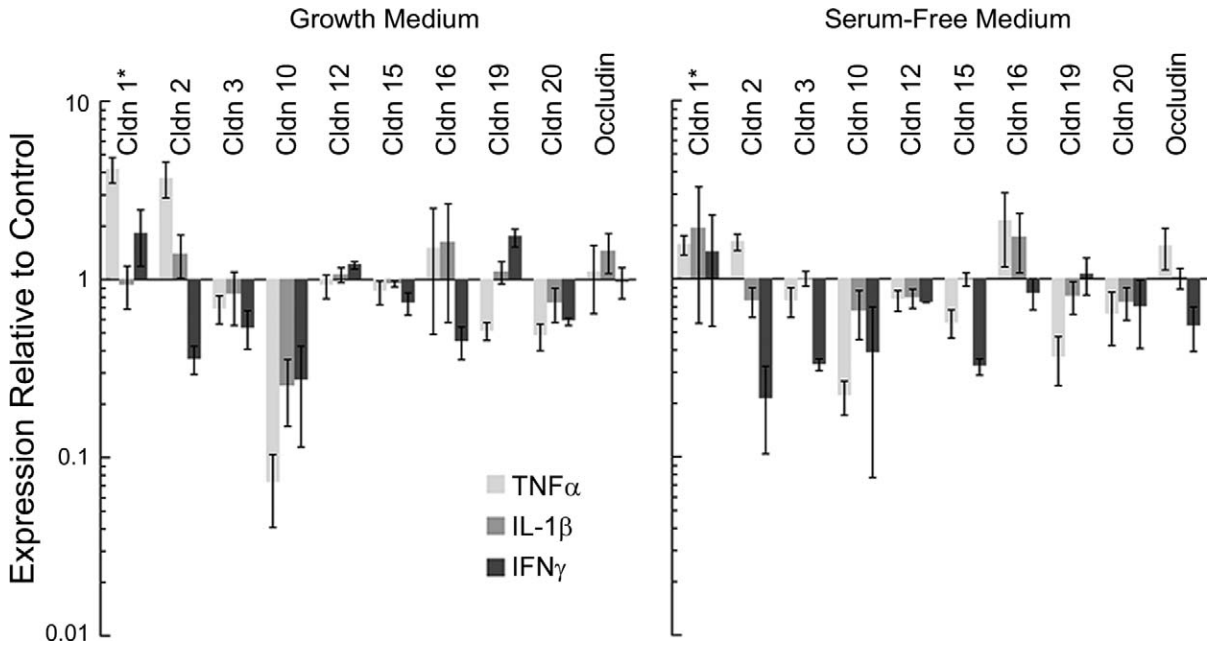

Figure 6. Effect of cytokines on gene expression. Cultures were maintained in GM or SFM-1 and incubated with the indicated cytokine for two days. The expression of mRNA was estimated by real-time RT-PCR. For each mRNA, expression relative to that mRNA in control cultures was calculated as described in Methods. (10 = 10× increase due to the cytokine; 0.1 = 10× decrease). Note that absolute expression levels for claudin-19 and occludin were >10× to 3000× higher than the other claudins, with claudin-16 having the lowest expression. Further, mRNA expression was unaffected by culture medium alone.[27] Cytokines had minimal effects on the expression of mRNAs for occludin and claudin-19. For the minor claudins, cytokines tended to lower the expression or had no effect. *Error bars for claudin-1 represent the range of two independent preparations of hfRPE. Remaining error bars represent the SE for three independent preparations of hfRPE. For each preparation, three cultures were measured.

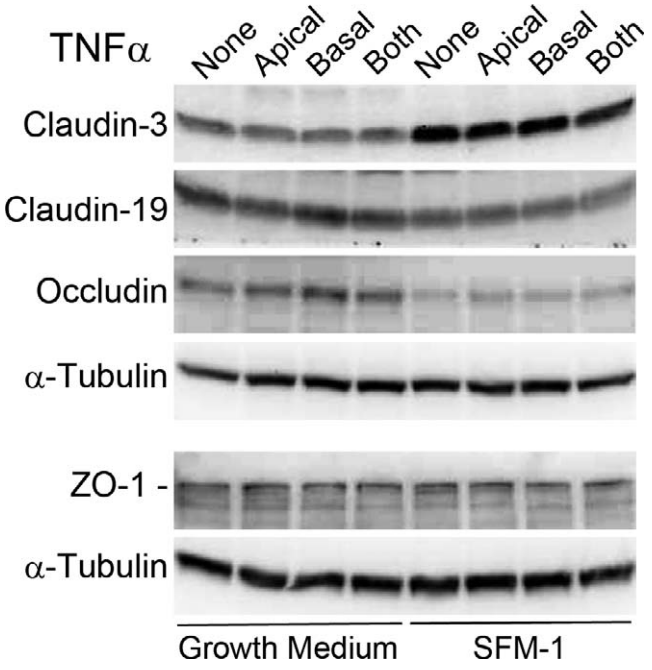

Figure 7. Expression of tight junctional proteins were affected minimally by TNFα in some donors. After a 48-hour exposure to TNFα, steady-state levels of claudin-3, claudin-19, and occludin decreased as much as 50% for many isolates of hfRPE. This donor provides an example of hfRPE whereby TNFα reduced TER by 80% with minimal effect on steady-state levels of these proteins or ZO-1. Note the two ZO-1 isoforms form the doublet indicated by the marker. The faster migrating band also was observed in nonimmune control samples (not shown).

hours, IL-1β had minimal effect. An effect of IFNγ on TER was observed occasionally and depended upon the donor (Table 1). By contrast, TNFα consistently caused a 70% to 95% decrease in TER regardless of donor. There was no evidence of a synergistic effect among the cytokines tested.

The effect of TNFα on TER was nonpolarized in cultures maintained in growth medium. However in SFM-1, the effect was minimal when TNFα was restricted to the basal medium chamber (Fig. 2A). The subcellular localization of the TNFα receptors, TNFR1 and TNFR2, could not be determined, because the immunofluorescent signal was too weak. In control cells the mRNA for TNFR1 was detected readily by qRT^2-PCR, but TNFR2 was evident only in trace amounts. In the presence of TNFα, mRNA for TNFR1 increased several fold, whereas mRNA for TNFR2 increased ~2 orders of magnitude. For TNFR1 in growth medium, TNFα had no effect unless the cytokine was included in the basal medium chamber, whereas in SFM-1 TNFα was effective in both medium chambers. The effect on TNFR2 was observed regardless of culture condition (Fig. 2B).

TNFα might induce apoptosis, which could reduce TER. However, we confirmed earlier reports[44] that this effect was not observed in hfRPE (Fig. 3). Because TNFR2 is associated with the inhibition of apoptosis, we also examined the cellular inhibitor of the apoptosis proteins, cIAP1 and cIAP2. The mRNA for both was induced by TNFα in either medium chamber (Fig. 2B).

To explore how cytokines might reduce TER via effects on tight junctions, we added cytokines to both medium chambers for 48 hours. Selectivity of the junctions for ions was studied by mounting the cultures in an Ussing chamber with media that inhibited transcellular transport. $BaCl_2$ was used to inhibit K^+ channels and the absence of bicarbonate was used to inhibit a second major class of ion transporters in RPE.[37–40] The

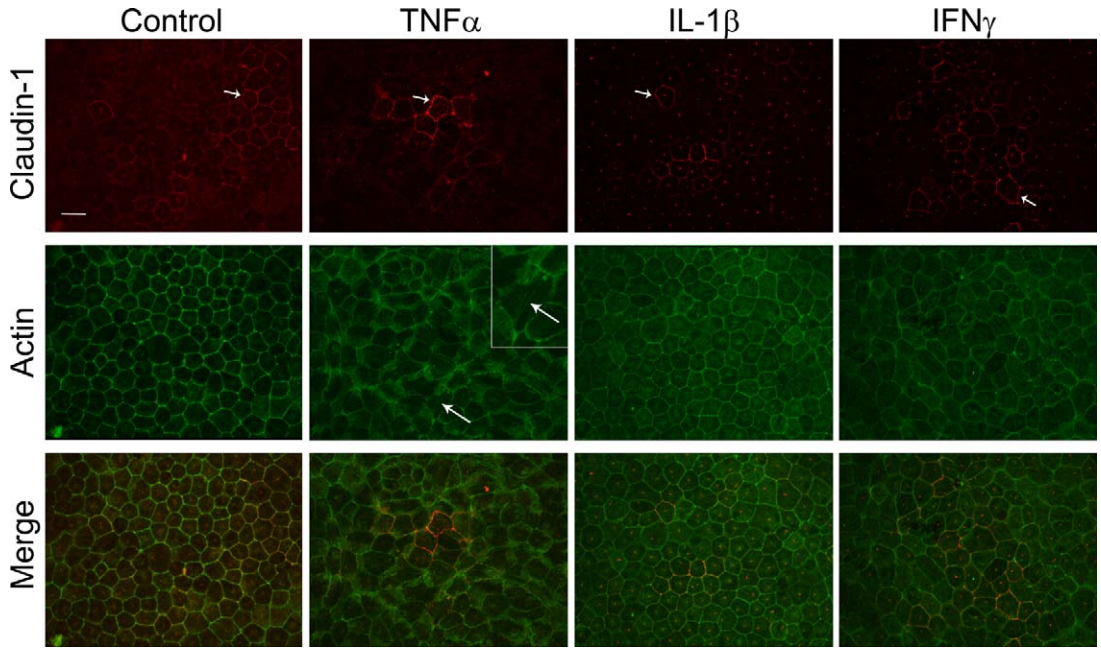

Figure 8. Effect of cytokines on the expression of claudin-1 and actin. Cells cultured in growth medium were incubated with the indicated cytokine for 2 days, labeled as described in Methods and imaged by confocal microscopy. The fluorescence channels were merged, and an MIP rendering was generated. Actin (*labeled green*) was expressed in apical junctional complexes and microvilli. Claudin-1 (*labeled red*) was expressed in a subset of cells (*short arrows*). An orange signal appeared where the two proteins co-localized. Claudin-1 and actin also co-localized with occludin (not shown). Although claudin-1 co-localized with actin in TNFα cells, the junctions often were tortuous. Stress fibers (*long arrows*) in the plane of the tight junction often were evident (cell indicated by *long arrow* is enlarged in the inset). There was no apparent effect of IL-1β and IFNγ when cells were cultured in growth medium. Similar results were obtained in SFM-1. *Bar*: 20 μm.

effectiveness of the protocol was demonstrated by the reduction of the TEP from ~2 mV to <0.6 mV. Permeation coefficients were calculated from the dilution and bi-ionic potentials for NaCl and KCl (Table 2). These potentials were determined from three cultures for each condition; representative data are shown in Figure 4. The effects of changing solutions were reversible, and the results were unaffected by the order in which the experiments were done.

In control cells, the tight junctions appeared to be slightly cation selective (Table 2). For Na^+, K^+, and Cl^-, the relative permeability coefficients for permeation across bare filters conformed to the expectation based on the diffusion of these ions in free solution: $Na^+ < Cl^- = K^+$.[45] In control cells, this relationship changed to $Na^+ = Cl^- < K^+$, as the ratio $P_{Na+/Cl-}$ increased relative to the bare filter. The ratio P_{K+}/P_{Na+} was the same for hfRPE and the bare filter. Consistent with the lower TER, the permeation coefficient for each of the ions tested was greater for the cells maintained in serum-free media, but their permeability relative to each other did not change.

The permeation of PEG_{550} was used to monitor the permeation of nonionic solutes that were slightly larger than the pore size of tight junctional strands.[27,46] A change in the permeation coefficient would indicate discontinuities in the network of tight junctional strands, or an increase in the rate of strands breaking and resealing. Despite the large difference in TER, there was no difference between the apparent permeation coefficient of PEG_{550} between control cells maintained in growth versus serum-free medium (Fig. 5). Neither IL-1β nor IFNγ had a substantial effect on permeation, although they had a slight, but statistically significant, decrease in permeation in the serum-free cultures. TNFα increased permeation of PEG_{550} substantially. There was no evidence of a synergistic effect among the cytokines tested.

Molecular Basis for the Effects of Cytokines

To examine the basis of these effects, we examined the expression of claudin and occludin mRNA by quantitative RT-PCR. Expression in the presence of cytokine for each mRNA was normalized to its expression in control conditions (Fig. 6). Accordingly, 1.0 represents no effect of cytokine on the expression of mRNA. As in earlier studies, we found that claudin-19 mRNA was expressed in control cells 10× to 3000× more than other claudin mRNAs.[27] Unlike the mRNAs for claudin-19 and occludin, the other claudin mRNAs were expressed near the limits of detection, which led to relatively large errors. The effect of cytokine often was less than 2×, which likely is not biologically significant. TNFα increased the expression of claudin-2, and decreased the expression of claudin-10 and claudin-19. IFNγ decreased the expression of claudin-2, claudin-3, and claudin-10. Like the effects of IFNγ on TER, the changes in claudin expression were variable. Consistent differences between culture media were not evident.

The effects of TNFα on claudin expression were variable. On immunoblots, TNFα could be shown to reduce claudin-3 or claudin-19 as much as 50% (not shown), but TNFα decreased the TER even when claudin or occludin expression was unaffected (Fig. 7). There was no apparent effect on the migration of occludin on polyacrylamide gels, which suggests that post-translational modifications were unaffected. The other cytokines had minimal effect (data not shown). There also was no effect on the steady-state levels of ZO-1 (Fig. 7).

Immunofluorescence revealed that TNFα did affect claudin-2 expression in subsets of RPE cells, but the other cytokines had minimal effects. As reported earlier, claudin-1 and claudin-2 were expressed in only subsets of cells (Figs. 8, 9). Cytokines had no overt effect on claudin-1 expression. In contrast,

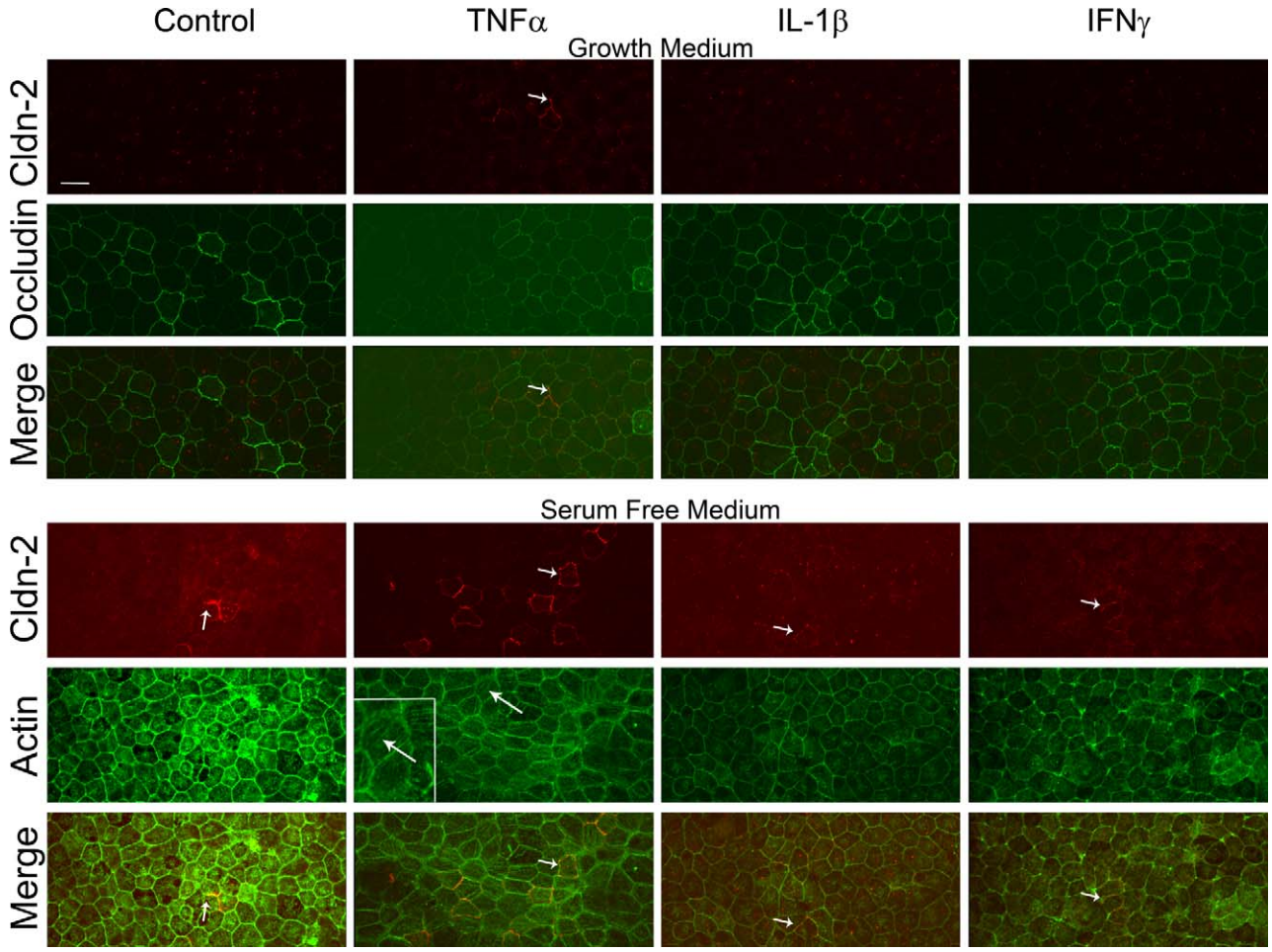

Figure 9. Effects of cytokines on the expression of claudin-2, occludin, and actin. Cells cultured in serum-free medium were incubated with the indicated cytokine for 2 days, labeled as described in Methods, and imaged by confocal microscopy. The fluorescence channels were merged, and an MIP rendering was generated. In both media, the immunofluorescent signal for claudin-2 (*red*) was below the threshold for detection in most cells. *Growth Medium*: cells cultured in GM were counter-labeled to reveal occludin (*green*). Claudin-2 could be detected in some cells (*short arrows*) in cultures exposed to TNFα. *Serum-free medium*: cells cultured in SFM-1 were counter-labeled to reveal actin (*green*) in apical stress fibers (*long arrows*) and along the apical junctional complex, which includes tight junctions. Claudin-2 (*short arrows*) occasionally was detected in all cultures, but with greater frequency in cultures that contained TNFα. *Bar*: 20 μm.

claudin-2–positive cells were rare in control cultures, and cultures treated with IL-1β and/or IFNγ; they were easier to find in cultures treated with TNFα. The claudin-2 induced by TNFα was incorporated into tight junctions (Fig. 10). Like claudin-1, cytokines had minimal effects on the expression of the major RPE claudins, claudin-3, and claudin-19 (Fig. 11).

An increase in claudin-2 expression could account for the decrease in TER. We tested this two ways. A siRNA specific for claudin-2 reduced expression of the mRNA 5- to 7-fold. Subsequent addition of TNFα could increase the residual claudin-2, but only to the levels observed in cells before the experiment (Fig. 12). Note that the slower migrating background protein observed in the presence of TNFα was unaffected by the siRNA. Nonetheless, TNFα continued to decrease the TER, as in cells untreated with this siRNA.

If the increased expression of claudin-2 was great enough to lower TER, it should increase the selectivity for cations,[47] but this was not observed (Table 2). To confirm this finding, an adenoviral vector was used to over express claudin-2. A vector that expressed green fluorescence protein had no effect on the permeability or selectivity of cultures maintained in SFM-1. Over expression of claudin-2 increased steady-state levels dramatically without affecting the expression of other claudins (Fig. 13A). Claudin-2 was found in the tight junctions of most cells. It reduced TER 30%, but in contrast to TNFα, increased the selectivity for cations ~3-fold (Fig. 13B, Table 3).

Notably, most of the cells in the TNFα cultures exhibited tortuous tight junctions with apical stress fibers (Figs. 8–10). A three-dimensional reconstruction of a cell in TNFα demonstrated that the apical junctional complexes were intact and that the actin stress fibers connected the apical junctional complex from one junction segment of the polygon to a segment on the opposite side of the cell (Fig. 10). (Note that actin also localizes to the adherens junction, which could not be resolved from the tight junction at this magnification. Together, these junctions form the apical junctional complex.)

Discussion

Properties of Human RPE Tight Junctions

Proinflammatory cytokines modulate transcellular fluxes across the hfRPE monolayer without disassembling tight junctions.[15] To understand how they might modulate the properties of tight junctions, we first consider the two claudins

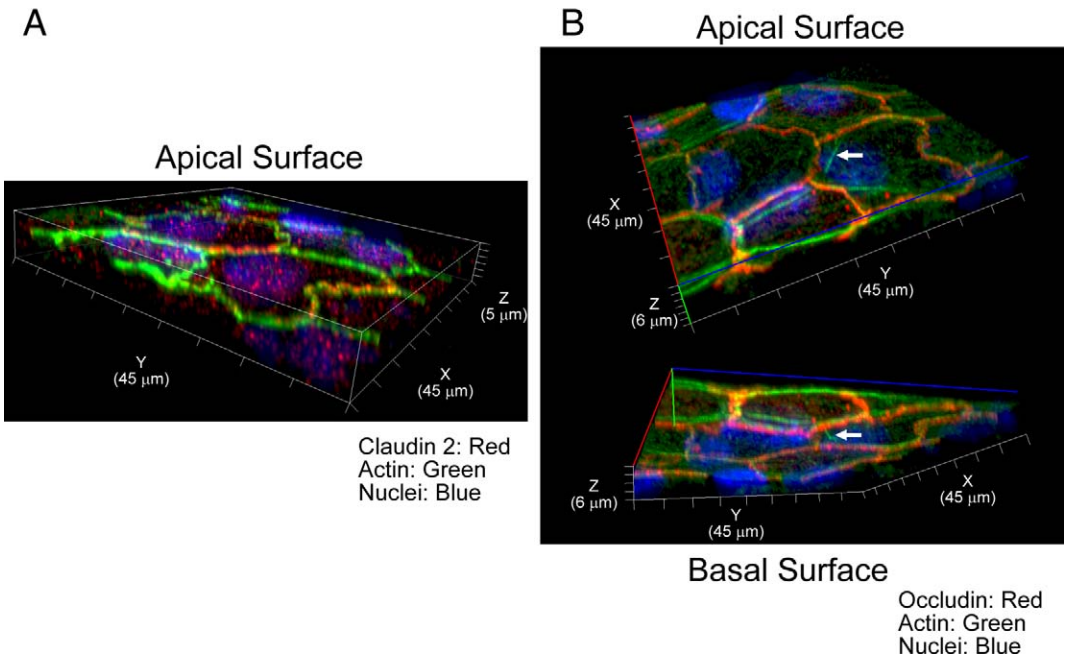

Figure 10. Localization of claudin-2 in tight junctions. Cells were cultured in GM with TNFα to generate claudin-2–positive cells, labeled as described in Methods. A three-dimensional rendering was generated from the confocal images. *White box*: indicates the thickness of the monolayer. The images were false colored to reveal the localization of the nucleus (*blue*), actin (*green*), claudin-2 (*red* in **A**), or occludin (*red* in **B**). (**A**) The image was tilted to view the apical surface and lateral cuts of the monolayer. The apical network of tight junctions was labeled with actin and claudin-2 (the occludin channel was turned off). Only two of the cells in this field expressed claudin-2, as revealed by the yellow-orange signal where actin and claudin-2 co-localize. (**B**) The same image as (**A**) was processed to reveal the co-localization of actin and occludin (the claudin-2 channel was turned off). Viewed from the apical surface, all the junctions were yellow due to the ubiquitous co-localization of occludin and actin. Actin also was observed in apical microvilli and stress fibers (*arrow*) that cross the cell to join a focal point on the apical junctional complex to a focal point of the complex on the opposite side of the cell. Viewed from the basal side, nuclei indicated the depth of the cell and the apical position of the junctional complex. Claudin-2, occludin, and actin co-localized in the apical junctional complex. Note the nonlinear path followed by the tight junction from one vertex of the polygon to the next. Similar results were obtained when ZO-1 was used to mark the tight junctions (not shown).

that are detectable in all cells of the human RPE monolayer: claudin-3 and claudin-19.

This report supports our earlier study that concluded claudin-19 is the dominant claudin in hfRPE.[27] That study showed that too little claudin-3 is present to form functional tight junctions on its own, as evidenced by siRNA knockdowns of either claudin-3 or claudin-19. The current study demonstrates that the selectivity of hfRPE differs from the prediction for a claudin-3 dominant junction. The relative permeation of ions in claudin-3 dominant junctions conform to Eisenman sequence IX ($Na^+ > K^+ > Li^+ > Rb^+ > Cs^+$) and $P_{Na+}/P_{Cl-} = 1.7$.[48,49] Eisenman sequences vary according to a pore's ability to reduce an ion's effective radius by removing water from its hydration sphere. The 11 Eisenman sequences represent pores of different "field strength." For sequence I each of these ions is hydrated fully as it passes through the pores (field strength is low), whereas for sequence XI all the ions are dehyrated fully. For hfRPE, K^+ was slightly more permeable than Na^+, which corresponds to Eisenman sequences I, II or VI, and $P_{Na+}/P_{Cl-} = 1.0$. Sequence 1 also characterizes ion diffusion coefficients in free solution, which would be the case if the monolayer were damaged. The data are inconsistent with a damaged monolayer, because the TER was high, the permeation coefficients of the ions and PEG were low and the monolayer formed an apical positive TEP in the absence of transport inhibitors. Further, $P_{Na+}/P_{Cl-} = 0.69$ in free solution. Small deflections of the dilution potential might reflect the liquid junction potential for the electrodes. However, this artifact also would affect measurements with the bare filter, with which the results ($P_{Na+}/P_{Cl-} = 0.77$) were close to the value predicted from free diffusion in solution. Therefore, hfRPE tight junctions exhibit a relatively hydrated, slightly cation-selective tight junction with a low permeability for ions and nonionic solutes regardless of whether it is maintained in growth medium or SFM-1.

Our results refine earlier characterizations of claudin-19 in which claudin-19 was expressed exogenously in cells whose own claudins already made a substantial contribution to the TER.[50] In MDCK II cells, cation-selective claudins masked the effect of claudin-19, whereas in anion-selective LLC-PK1 cells, claudin-19 selectively reduced the permeability of Cl^-. The current study indicates that claudin-19 decreases the permeation coefficient for anions and cations, but may be slightly selective for cations.

A second aspect of selectivity concerns large nonionic solutes. The ability to regulate the permeation of ionic and nonionic solutes semi-independently is explained by the following model.[13,46] Ions and small ionic solutes (Stokes radius <4 Å) pass through pores in the tight junctional strands, but larger solutes rely on the breaking and resealing of tight junctional strands.[13,46] Because PEG_{550} (average Stokes radius = 5.1 Å) is larger than the estimated pore size of junctional strands,[46] our data suggested that the rate of strand breaking and resealing was the same in growth medium and SFM-1.

Even though selectivity was unaffected by culture medium, the TER and permeation coefficient of ions was affected. Our previous study showed that the increase in TER was caused by the presence of serum in the apical medium chamber, and correlated with an increase in the expression of occludin.[27] Rather than strand-breaking and resealing, our current study suggests that occludin might regulate permeability by influ-

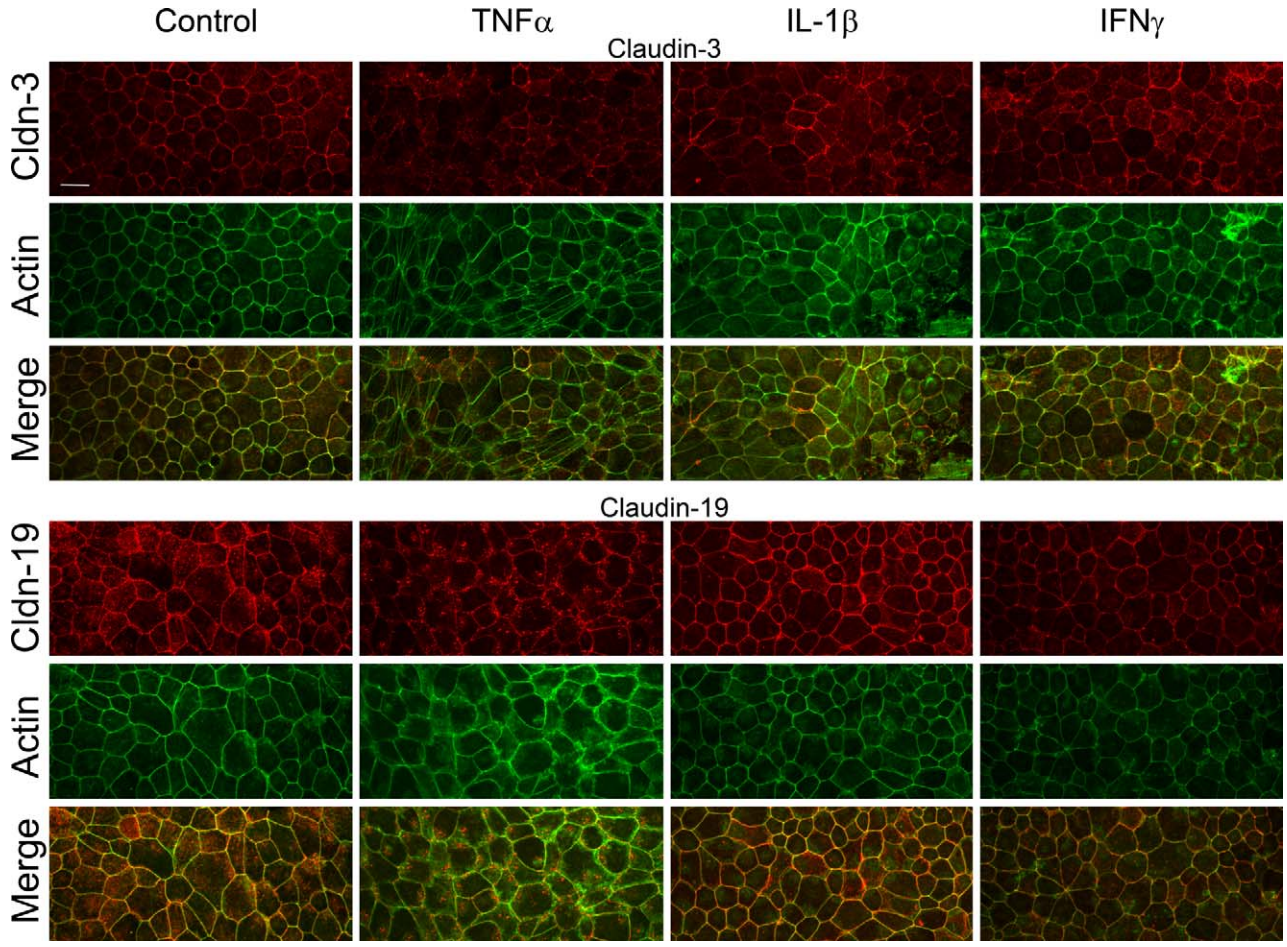

Figure 11. Effect of cytokines on the expression of claudin-3 and claudin-19. Cells cultured in GM were incubated in the indicated cytokine for 2 days, labeled as described in Methods and imaged by confocal microscopy. The fluorescence channels were merged, and an MIP rendering was generated. In control cultures and cultures incubated in IFNγ, most of the junctions appear orange-yellow due to the co-localization of claudin-3, or claudin-19 (*labeled red*) and actin (*labeled green*). Similar results were obtained in SFM-1. *Bar*: 20 μm.

encing the density of pores in the tight junctional strands or the rate of pore opening and closing. This is consistent with the observation that occludin regulates permeability rather than selectivity.[51]

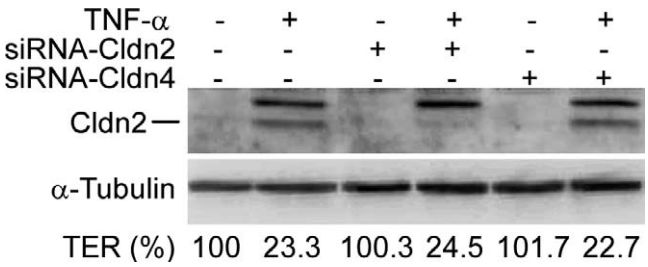

Figure 12. Effect of TNFα with reduced levels of claudin-2. Cells were transfected with siRNA against claudin-2 (*Cldn2*) or against a claudin not expressed by hfRPE, claudin-4 (*Cldn4*). After claudin-2 levels were reduced (day 9), the indicated cultures were incubated with TNFα for 48 hours. With claudin-2 siRNA, the mRNA levels for claudin-2 were reduced 5 to 7× during the exposure to TNFα siRNA had no effect on TER. The TER, expressed as a percentage of the control, is the average of three cultures. The TER of the control cells was 1338 $\Omega \times cm^2$. The SE was less than 5%. Note that a slower migrating, cross-reacting background protein was induced by TNFα. This background protein was not affected by either siRNA.

Effects of TNFα

TNFα increased substantially the paracellular permeation coefficients for ions and larger nonionic tracers alike with minimal effect on selectivity. Unlike the rapid effect of IFNγ on Cl^- and fluid transport,[15,16] the effect of TNFα developed slowly over 24 hours. In SFM-1, TER decreased only when TNFα was presented to the apical membrane.

In some epithelia, TNFα decreased TER via apoptosis and/or redistribution of tight junction proteins.[17–20,52] Our study confirmed earlier reports[44] that TNFα had little or no effect on apoptosis in RPE. Additionally, we showed that TNFα induced the expression of the mRNAs for TNFR2, a promoter of cell survival and proliferation,[53,54] and cIAP1 and cIAP2, inhibitors of apoptosis.[55]

TNFα reduced the TER without affecting the expression of claudins, occludin, or ZO-1. Although decreases in the expression of these proteins were observed in RPE derived from several donors, the decrease was not obligatory for the effect of TNFα on TER. Even in cultures where decreased expression occurred, the junctions remained intact, as demonstrated by the presence of a TER, TEP, and the co-localization of actin, ZO-1, occludin, claudin-3, and claudin-19 in an apical junctional complex. This contradicts a study where TNFα caused junctions to disassemble and leave gaps in monolayers of ARPE19 cells, a human RPE cell line.[56] In that

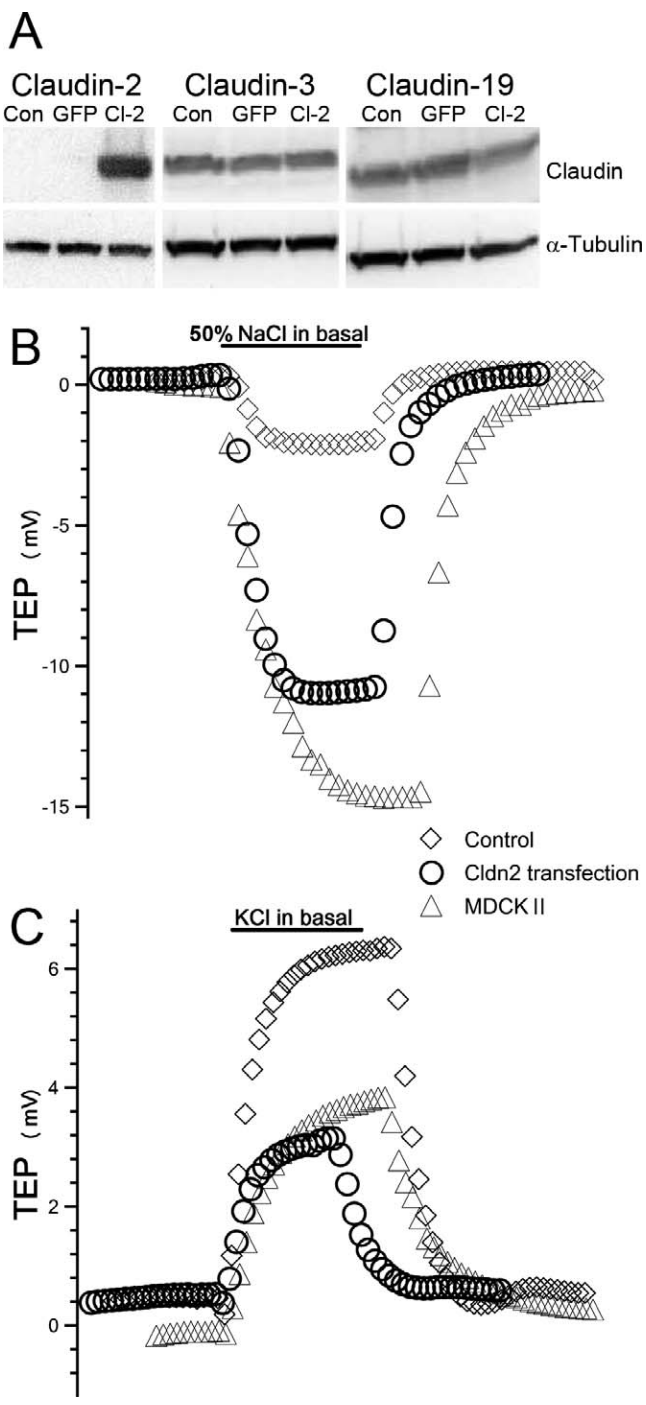

Figure 13. Overexpression of claudin-2 changes the selectivity of RPE tight junctions. (**A**) hfRPE was uninfected (*con*) or infected with an adenoviral vector that expressed either green fluorescent protein (*GFP*) or claudin-2 (*Cl-2*). After one day protein was extracted and immunoblotted for claudin-2, claudin-3, or claudin-19. Expression of claudin-2 increased, but expression of the other claudins was unaffected. (**B**) Dilution and (**C**) bi-ionic potentials were compared for Adeno-GFP infected (*Con* ◇) and Adeno-Claudin-2 infected (*Cldn2* ○) hfRPE. Claudin-2 rich Madin-Darby Canine Kidney 2 cells (*MDCK II* △) are included as a reference. *Bar*: indicates when NaCl solution in the basal chamber was replaced with KCl or 50% NaCl solution. Data were collected every 10 seconds; 1.0-minute intervals are indicated on the graph. Each trace is representative of three experiments. The data were used to calculate the permeation coefficients listed in Table 3.

report, ARPE19 was cultured in a high serum-containing media in which ARPE19 tight junctions can be rudimentary and claudin-19 is not evident.[13,29,57] Therefore, it is not possible to compare our two studies.

The increase in TER might be explained by the increase of claudin-2, but several lines of evidence argue against this. Claudin-2 increases TER by increasing cation selectivity.[47] When we overexpressed claudin-2, TER did decrease and the permeation coefficients for cations increased more than anions. However, TNFα had no effect on selectivity. Further, reducing claudin-2 expression by siRNA failed to inhibit the effects of TNFα. Nonetheless, the ability of TNFα to increase claudin-2 expression in a subset of cells suggests that TNFα could affect selectivity regionally, if these cells were segregated in a particular region of the RPE monolayer.

A more likely explanation for the decrease in TER is the monolayer wide effect of TNFα on the structure of tight junctions. The tortuosity of the tight junctions in the plane of the monolayer increased, which would lower TER by increasing the linear length of the junctions relative to area of the monolayer.[58] The TER also could be decreased by the tension placed upon the tight junctions by apical stress fibers that were induced by TNFα. An analogous mechanism decreased the TER in intestinal cells.[59] The mechanism of action requires further study.

Mechanistic studies should include the signaling pathway of TNFα. Our earlier study of hfRPE showed how serum in the apical medium chamber raises TER to hyperphysiologic levels.[27] In our current study, SFM-1 polarized one of the effects of TNFα. TNFα increased the expression of its receptors and the cIAPs from both sides of the monolayer, whereas the effect on TER was triggered only by apical TNFα. These findings imply that the distribution of the TNFα receptors is nonpolarized, but that the signaling pathways coupled to them are polarized.

We did not observe the synergistic effects on tight junctions that have been described for IFNγ and TNFα in other epithelia.[20,25,26] We confirmed an earlier report[15] that a 24-hour exposure to IFNγ would reduce TER slightly, but only in a subset of donors. Therefore, TNFα and IFNγ affect the barrier functions of RPE by distinct mechanisms that include tight junctions and membrane transport. The mechanisms that coordinate tight junctions and membrane transport deserve greater attention if we are to understand the role of the outer blood-retinal barrier in health and disease.

IL-1β had no effect when given alone or in combination with the other cytokines tested. In contrast, IL-1β was reported to disrupt tight junctions in the ARPE19 cell line concomitant with a decrease in occludin expression, but an increase in claudin-1.[14] For reasons noted earlier, the tight junctions in those culture conditions were quite different from hfRPE. In low-serum media that optimized the differentiation of ARPE19, ARPE19 more resembled diseased or aged RPE, whereas hfRPE more resembled normal RPE.[60] Therefore, our findings might be most relevant to early stages of innate inflammation when tight junctions are functionally intact.

We believe SFM-1 offers several advantages for studying hfRPE. The absence of serum on the apical side of the monolayer reduces TER to physiologic levels.[27] Under these conditions, a polarized response to the presence of TNFα was revealed. This finding raises the hypothesis that the immune response of RPE might vary according to the challenges presented by different pathologies. When presented from the choroid, TNFα would protect against apoptosis and maintain a tight monolayer that allows IFNγ to increase fluid absorption. In contrast, TNFα in the subretinal space would preserve a leaky monolayer that enables free diffusion between the choriocapillaris and subretinal space.

Table 3. Effect of Claudin-2 Over-Expression on Ion Selectivity

	Apparent R_{tj} ($\Omega \times cm^2$)	TEP (mV)	Permeation Coefficient ($P \times 10^6$cm/s)			Permeation Ratio		
			Na^+	K^+	Cl^-	Na^+/Cl^-	K^+/Cl^-	K^+/Na^+
GFP	360 ± 30	0.1 ± 0.2	3.9 ± 0.1	5.6 ± 0.1	3.0 ± 0.1	1.32 ± 0.05	1.88 ± 0.01	1.43 ± 0.09
Claudin-2	240 ± 2*	0.16 ± 0.05	8.4 ± 0.9	9.4 ± 0.9	1.9 ± 0.1	4.4 ± 0.6	5.0 ± 0.7	1.13 ± 0.01
MDCK II	47 ± 4†	0.03 ± 0.06	48 ± 3†	56 ± 4†	4 ± 2	15 ± 5†	17 ± 6†	1.15 ± 0.02

Cells were infected for 24 hours with adenoviral vectors that expressed either GFP or Claudin-2. For reference, experiments include MDCK II cells, which are rich in claudin-2 but lack claudin-3 and claudin-19.[50] Measurements were made in the presence of transport inhibitors, as described in the legend to Table 2.

* $P < 0.05$ compared to the control (GFP).

† $P < 0.05$ compared to the control (Claudin-2).

Acknowledgments

Sheldon Miller and Arvydas Maminishkis provided helpful suggestions and primary cultures of hfRPE. Mikio Furuse provided antibodies to claudin-19 and Lina Li provided expert technical assistance.

References

1. Yang D, Elner SG, Bian ZM, Till GO, Petty HR, Elner VM. Pro-inflammatory cytokines increase reactive oxygen species through mitochondria and NADPH oxidase in cultured RPE cells. *Exp Eye Res*. 2007;85:462–472.
2. Demircan N, Safran BG, Soylu M, Ozcan AA, Sizmaz S. Determination of vitreous interleukin-1 (IL-1) and tumour necrosis factor (TNF) levels in proliferative diabetic retinopathy. *Eye (Lond)*. 2006;20:1366–1369.
3. Foxman EF, Zhang M, Hurst SD, et al. Inflammatory mediators in uveitis: differential induction of cytokines and chemokines in Th1- versus Th2-mediated ocular inflammation. *J Immunol*. 2002;168:2483–2492.
4. Takase H, Futagami Y, Yoshida T, et al. Cytokine profile in aqueous humor and sera of patients with infectious or noninfectious uveitis. *Invest Ophthalmol Vis Sci*. 2006;47:1557–1561.
5. Cousins SW, Espinosa-Heidmann DG, Csaky KG. Monocyte activation in patients with age-related macular degeneration: a biomarker of risk for choroidal neovascularization? *Arch Ophthalmol*. 2004;122:1013–1018.
6. Mo JS, Matsukawa A, Ohkawara S, Yoshinaga M. Involvement of TNF alpha, IL-1 beta and IL-1 receptor antagonist in LPS-induced rabbit uveitis. *Exp Eye Res*. 1998;66:547–557.
7. Oh H, Takagi H, Takagi C, et al. The potential angiogenic role of macrophages in the formation of choroidal neovascular membranes. *Invest Ophthalmol Vis Sci*. 1999;40:1891–1898.
8. Frey TA, Antonetti DA. Alterations to the blood-retinal barrier in diabetes: cytokines and reactive oxygen species. *Antioxid Redox Signal*. 2011;15:1271–1284.
9. Zheng M, Atherton SS. Cytokine profiles and inflammatory cells during HSV-1-induced acute retinal necrosis. *Invest Ophthalmol Vis Sci*. 2005;46:1356–1363.
10. Vinores SA, Derevjanik NL, Ozaki H, Okamoto N, Campochiaro PA. Cellular mechanisms of blood-retinal barrier dysfunction in macular edema. *Doc Ophthalmol*. 1999;97:217–228.
11. Xu HZ, Le YZ. Significance of outer blood-retina barrier breakdown in diabetes and ischemia. *Invest Ophthalmol Vis Sci*. 2011;52:2160–2164.
12. Holtkamp GM, Kijlstra A, Peek R, de Vos AF. Retinal pigment epithelium-immune system interactions: cytokine production and cytokine-induced changes. *Prog Retin Eye Res*. 2001;20:29–48.
13. Rizzolo LJ, Peng S, Luo Y, Xiao W. Integration of tight junctions and claudins with the barrier functions of the retinal pigment epithelium. *Prog Retin Eye Res*. 2011;30:296–323.
14. Abe T, Sugano E, Saigo Y, Tamai M. Interleukin-1beta and barrier function of retinal pigment epithelial cells (ARPE-19): aberrant expression of junctional complex molecules. *Invest Ophthalmol Vis Sci*. 2003;44:4097–4104.
15. Li R, Maminishkis A, Banzon T, et al. IFN{gamma} regulates retinal pigment epithelial fluid transport. *Am J Physiol Cell Physiol*. 2009;297:C1452–C1465.
16. Shi G, Maminishkis A, Banzon T, et al. Control of chemokine gradients by the retinal pigment epithelium. *Invest Ophthalmol Vis Sci*. 2008;49:4620–4630.
17. Schmitz H, Fromm M, Bentzel CJ, et al. Tumor necrosis factor-alpha (TNFalpha) regulates the epithelial barrier in the human intestinal cell line HT-29/B6. *J Cell Sci*. 1999;112:137–146.
18. Marano CW, Lewis SA, Garulacan LA, Soler AP, Mullin JM. Tumor necrosis factor-α increases sodium and chloride conductance across the tight junction of CACO-2 BBE, a human intestinal epithelial cell line. *J Memb Biol*. 1998;161:263–274.
19. Mullin JM, Marano CW, Laughlin KV, Nuciglio M, Stevenson BR, Soler AP. Different size limitations for increased transepithelial paracellular solute flux across phorbol ester and tumor necrosis factor-treated epithelial cell sheets. *J Cell Physiol*. 1997;171:226–233.
20. Bruewer M, Luegering A, Kucharzik T, et al. Proinflammatory cytokines disrupt epithelial barrier function by apoptosis-independent mechanisms. *J Immunol*. 2003;171:6164–6172.
21. Sugi K, Musch MW, Field M, Chang EB. Inhibition of Na+,K+-ATPase by interferon gamma down-regulates intestinal epithelial transport and barrier function. *Gastroenterology*. 2001;120:1393–1403.
22. Youakim A, Ahdieh M. Interferon-gamma decreases barrier function in T84 cells by reducing ZO-1 levels and disrupting apical actin. *Am J Physiol*. 1999;276:G1279–G1288.
23. Oshima T, Laroux FS, Coe LL, et al. Interferon-gamma and interleukin-10 reciprocally regulate endothelial junction integrity and barrier function. *Microvasc Res*. 2001;61:130–143.
24. Ahdieh M, Vandenbos T, Youakim A. Lung epithelial barrier function and wound healing are decreased by IL-4 and IL-13 and enhanced by IFN-gamma. *Am J Physiol Cell Physiol*. 2001;281:C2029–C2038.
25. Coyne CB, Vanhook MK, Gambling TM, Carson JL, Boucher RC, Johnson LG. Regulation of airway tight junctions by proinflammatory cytokines. *Mol Biol Cell*. 2002;13:3218–3234.
26. Fish SM, Proujansky R, Reenstra WW. Synergistic effects of interferon gamma and tumour necrosis factor alpha on T84 cell function. *Gut*. 1999;45:191–198.
27. Peng S, Rao VS, Adelman RA, Rizzolo LJ. Claudin-19 and the barrier properties of the human retinal pigment epithelium. *Invest Ophthalmol Vis Sci*. 2011;52:1392–1403.

28. Booij JC, ten Brink JB, Swagemakers SMA, et al. A new strategy to identify and annotate human RPE-specific gene expression. *PLoS ONE*. 2010;5:e9341.
29. Strunnikova NV, Maminishkis A, Barb JJ, et al. Transcriptome analysis and molecular signature of human retinal pigment epithelium. *Hum Mol Genet*. 2010;19:2468–2486.
30. Konrad M, Schaller A, Seelow D, et al. Mutations in the tight-junction gene claudin 19 (CLDN19) are associated with renal magnesium wasting, renal failure, and severe ocular involvement. *Am J Hum Genet*. 2006;79:949–957.
31. Antonell A, Del Campo M, Magano LF, et al. Partial 7q11.23 deletions further implicate GTF2I and GTF2IRD1 as the main genes responsible for the Williams-Beuren syndrome neurocognitive profile. *J Med Genet*. 2010;47:312–320.
32. Castelo-Branco M, Mendes M, Sebastião AR, et al. Visual phenotype in Williams-Beuren syndrome challenges magnocellular theories explaining human neurodevelopmental visual cortical disorders. *J Clin Invest*. 2007;117:3720–3729.
33. Maminishkis A, Chen S, Jalickee S, et al. Confluent monolayers of cultured human fetal retinal pigment epithelium exhibit morphology and physiology of native tissue. *Invest Ophthalmol Vis Sci*. 2006;47:3612–3624.
34. Peng S, Adelman RA, Rizzolo LJ. Minimal effects of VEGF and anti-VEGF drugs on the permeability or selectivity of RPE tight junctions. *Invest Ophthalmol Vis Sci*. 2010;51:3216–3225.
35. Gamm DM, Melvan JN, Shearer RL, et al. A novel serum-free method for culturing human prenatal retinal pigment epithelial cells. *Invest Ophthalmol Vis Sci*. 2008;49:788–799.
36. Reuss L. Tight junction permeability to ions and water. In: Cereijido M, Anderson JM, eds. *Tight Junction, 2nd ed*. Boca Raton, FL: CRC Press; 2001:61–88.
37. Yang D, Zhang X, Hughes BA. Expression of inwardly rectifying potassium channel subunits in native human retinal pigment epithelium. *Exp Eye Res*. 2008;87:176–183.
38. Doring F, Derst C, Wischmeyer E, et al. The epithelial inward rectifier channel Kir7.1 displays unusual K+ permeation properties. *J Neurosci*. 1998;18:8625–8636.
39. Krapivinsky G, Medina I, Eng L, Krapivinsky L, Yang Y, Clapham DE. A novel inward rectifier K+ channel with unique pore properties. *Neuron*. 1998;20:995–1005.
40. Adijanto J, Banzon T, Jalickee S, Wang NS, Miller SS. CO_2-induced ion and fluid transport in human retinal pigment epithelium. *J Gen Physiol*. 2009;133:603–622.
41. Kimizuka H, Koketsu K. Ion transport through cell membrane. *J Theor Biol*. 1964;6:290–305.
42. Yu AS, Cheng MH, Angelow S, et al. Molecular basis for cation selectivity in claudin-2-based paracellular pores: identification of an electrostatic interaction site. *J Gen Physiol*. 2009;133:111–127.
43. Livak KJ, Schmittgen TD. Analysis of relative gene expression data using real-time quantitative PCR and the 2(-delta delta C(T)) method. *Methods*. 2001;25:402–408.
44. Yang P, McKay BS, Allen JB, Jaffe GJ. Effect of NF-kappa B inhibition on TNF-alpha-induced apoptosis in human RPE cells. *Invest Ophthalmol Vis Sci*. 2004;45:2438–2446.
45. Powell DW. Barrier function of epithelia. *Am J Physiol*. 1981;241:G275–G288.
46. Van Itallie CM, Holmes J, Bridges A, et al. The density of small tight junction pores varies among cell types and is increased by expression of claudin-2. *J Cell Sci*. 2008;121:298–305.
47. Amasheh S, Meiri N, Gitter AH, et al. Claudin-2 expression induces cation-selective channels in tight junctions of epithelial cells. *J Cell Sci*. 2002;115:4969–4976.
48. Milatz S, Krug SM, Rosenthal R, et al. Claudin-3 acts as a sealing component of the tight junction for ions of either charge and uncharged solutes. *Biochim Biophys Acta*. 2010;1798:2048–2057.
49. Eisenman G, Horn R. Ionic selectivity revisited: the role of kinetic and equilibrium processes in ion permeation through channels. *J Membr Biol*. 1983;76:197–225.
50. Hou J, Renigunta A, Konrad M, et al. Claudin-16 and claudin-19 interact and form a cation-selective tight junction complex. *J Clin Invest*. 2008;118:619–628.
51. Cummins PM. Occludin: one protein, many forms. *Mol Cell Biol*. 2012;32:242–250.
52. Marchiando AM, Shen L, Graham WV, et al. The epithelial barrier is maintained by in vivo tight junction expansion during pathologic intestinal epithelial shedding. *Gastroenterology*. 2011;140:1208–1218.
53. Al-Lamki RS, Wang J, Vandenabeele P, et al. TNFR1- and TNFR2-mediated signaling pathways in human kidney are cell type-specific and differentially contribute to renal injury. *FASEB J*. 2005;19:1637–1645.
54. Luo D, Luo Y, He Y, et al. Differential functions of tumor necrosis factor receptor 1 and 2 signaling in ischemia-mediated arteriogenesis and angiogenesis. *Am J Pathol*. 2006;169:1886–1898.
55. Deveraux QL, Roy N, Stennicke HR, et al. IAPs block apoptotic events induced by caspase-8 and cytochrome c by direct inhibition of distinct caspases. *EMBO J*. 1998;17:2215–2223.
56. Narayan S, Prasanna G, Krishnamoorthy RR, Zhang X, Yorio T. Endothelin-1 synthesis and secretion in human retinal pigment epithelial cells (ARPE-19): differential regulation by cholinergics and TNF-alpha. *Invest Ophthalmol Vis Sci*. 2003;44:4885–4894.
57. Luo Y, Zhuo Y, Fukuhara M, Rizzolo LJ. Effects of culture conditions on heterogeneity and the apical junctional complex of the ARPE-19 cell line. *Invest Ophthalmol Vis Sci*. 2006;47:3644–3655.
58. Claude P. Morphological factors influencing transepithelial permeability: a model for the resistance of the zonula occludens. *J Membr Biol*. 1978;39:219–232.
59. Madara JL, Moore R, Carlson S. Alteration of intestinal tight junction structure and permeability by cytoskeletal contraction. *Am J Physiol*. 1987;253:C854–C861.
60. Ablonczy Z, Dahrouj M, Tang PH, et al. Human retinal pigment epithelium cells as functional models for the RPE in vivo. *Invest Ophthalmol Vis Sci*. 2011;52:8614–8620.